

# Experimental conditions for observation of electron-hole superfluidity in GaAs heterostructures

Samira Saberi-Pouya,<sup>1</sup> Sara Conti,<sup>1,2</sup> Andrea Perali,<sup>3</sup> Andrew F. Croxall,<sup>4</sup>

Alexander R. Hamilton,<sup>5</sup> François M. Peeters,<sup>1</sup> and David Neilson<sup>1,5</sup>

<sup>1</sup>*Department of Physics, University of Antwerp, Groenenborgerlaan 171, 2020 Antwerpen, Belgium*

<sup>2</sup>*Physics Division, School of Science and Technology, Università di Camerino, 62032 Camerino (MC), Italy*

<sup>3</sup>*Supernano Laboratory, School of Pharmacy, Università di Camerino, 62032 Camerino (MC), Italy*

<sup>4</sup>*Cavendish Laboratory, University of Cambridge, J.J. Thomson Avenue, Cambridge CB3 0HE, United Kingdom*

<sup>5</sup>*ARC Centre of Excellence for Future Low Energy Electronics Technologies, School of Physics,*

*The University of New South Wales, Sydney, New South Wales 2052, Australia*

(Dated: March 3, 2020)

The experimental parameter ranges needed to generate superfluidity in optical and drag experiments in GaAs double quantum wells are determined, using a formalism that includes self-consistent screening of the Coulomb pairing interaction in the presence of the superfluid. The very different electron and hole masses in GaAs make this a particularly interesting system for superfluidity, with exotic superfluid phases predicted in the BCS-BEC crossover regime. We find that the density and temperature ranges for superfluidity cover the range for which optical experiments have observed indications of superfluidity, but that existing drag experiments lie outside the superfluid range. We also show that for samples with low mobility with no macroscopically connected superfluidity, if the superfluidity survives in randomly distributed localized pockets, standard quantum capacitance measurements could detect these pockets.

While Bose Einstein Condensation (BEC) and the BCS-BEC crossover phenomena in superfluidity have been extensively studied for ultracold Fermi atoms,<sup>1-3</sup> it is probable that practical applications will instead be based on superfluidity in solid state devices. Existence of superfluidity in coupled atomically-flat layers in semiconductor heterostructures has been theoretically predicted,<sup>4,5</sup> while recent observations of dramatically enhanced tunneling at equal densities in electron-hole double bilayer sheets of graphene<sup>6,7</sup> and in double monolayers of transition metal dichalcogenide monolayers<sup>8,9</sup> are strong experimental indications for electron-hole condensation.<sup>10</sup>

Electron-hole superfluidity and the BCS-BEC crossover was first proposed for an excitonic system in a conventional semiconductor heterostructure of double quantum-wells in GaAs.<sup>11</sup> This was based on extensions of earlier work on exciton condensation.<sup>12-15</sup> To block electron-hole recombination, Refs. 14,15 proposed spatially separating the electrons and holes in a heterostructure consisting of two layers separated by an insulating barrier.

Superfluidity in GaAs quantum-wells differs in significant ways from superfluidity in coupled atomically-flat layers. The large band gap in GaAs eliminates the multicondensate effects and multiband screening that are important in graphene,<sup>16</sup> and the low-lying conduction and valence bands are nearly parabolic, and not dependent on gate potentials.

However it is the widely different electron and hole effective masses that provides the most dramatic contrast of superfluidity in GaAs compared with superfluidity in other solid state devices. In GaAs the masses differ by a large factor: we take  $m_e^* = 0.067m_e$  and  $m_h^* = 0.3m_e$ . Not only does this have significant consequences for the superfluid properties,<sup>17</sup> but also for the screening responses of the electrons and holes, which are significantly different from the equal mass case. In ultracold atomic gases, Dy-K Fermi mixtures have been used to explore the physics of mass-imbalanced strongly interacting Fermi-Fermi mixtures.<sup>18</sup>

The large mass difference makes double quantum wells in GaAs a solid state system uniquely suitable for generating and enhancing exotic superfluid phases that span the BCS-BEC crossover.<sup>19</sup> Such phases can also be expected in mass-imbalanced ultracold atomic gas Fermi mixtures,<sup>20</sup> but only at currently inaccessible temperatures,<sup>21</sup>  $T_c \lesssim 50$  nK. The phases include the Fulde-Ferrell-Larkin-Ovchinnikov (FFLO) phase<sup>22</sup> and the Sarma phase with two Fermi surfaces (breached pair phase).<sup>23</sup> For GaAs, our estimates for transition temperatures to the FFLO phase are readily accessible experimentally,  $T_c \sim 0.2 - 0.5$  K. Potentially even more exciting is the possibility of a Larkin-Ovchinnikov supersolid phase when the masses are unequal.<sup>24,25</sup>

For these reasons, experimental realization of superfluidity in GaAs quantum wells is of great interest. A major challenge facing experiments is that electron-hole superfluidity in double layer systems is exclusively a low density phenomenon, because strong screening of the long-range Coulomb pairing interactions suppresses superfluidity above an onset density  $n_0$ , and this is low.<sup>4,16,26,27</sup> Nevertheless, there are reports suggesting possible experimental signatures of electron-hole superfluid condensation in GaAs double quantum-wells. Some signatures are based on optical observations of indirect exciton luminescence,<sup>28-31</sup> while others are based on transport measurements of Coulomb drag.<sup>32,33</sup>

In this paper we map out the parameter space for GaAs double quantum well heterostructures to determine where electron-hole superfluidity is favored. Important parameters are the widths  $w$  of the quantum wells, the thickness  $t_B$  of the  $\text{Al}_x\text{Ga}_{1-x}\text{As}$  insulating barrier, the densities in the wells  $n$  (assumed equal), and any perpendicular electric fields. The distance between the peaks of the density distributions of the electrons and holes must be calculated, and is usually not simply the distance between the centers of the quantum wells. By establishing the parameter ranges expected for superfluidity, we are able to provide independent corroborative support for the reported experimental signatures suggesting superfluidity.

Existing optical experiments generally use samples with quantum wells and barriers which are narrower than in samples for transport measurements. A major reason is that a problem arises for transport with the narrower wells from interface roughness scattering caused by Al atoms in the insulating barrier diffusing into the well regions. Interface roughness scattering dramatically reduces the mobility, which is an essential consideration for transport measurements. Also, in optical measurements, electron-hole pairs are optically excited in a quantum well and then spatially separated across the barrier by means of a perpendicular electric field. Thus barriers are generally thinner than those for transport experiments, so the coupling of the electron-hole pairs tends to be stronger for optical measurements.

For the optical experiments we consider the samples from Refs. 28–30, with 8 nm GaAs quantum wells separated by a 4 nm barrier of  $\text{Al}_x\text{Ga}_{1-x}\text{As}$ , and Ref. 31 with 12 nm wells and a 1.1 nm AlAs barrier. Techniques to optically identify macroscopic spatial coherence were: the appearance in photoluminescence measurements of bright localized spots with enhanced luminescence at fixed points on the sample;<sup>28</sup> the abrupt appearance of a sharp inter-well exciton line in the photoluminescence spectra;<sup>31</sup> an abrupt increase in the amplitude of interference fringes using a Mach-Zehnder interferometer<sup>29</sup> indicating a strong enhancement of the exciton coherence length; quenching of photoluminescence emission as a manifestation of optically-dark exciton condensation.<sup>30</sup> Indications of coherent condensation were observed at temperatures of a few Kelvin at carrier densities of a few  $10^{10} \text{ cm}^{-2}$ .

From the samples used in the Coulomb drag experiments,<sup>32,33</sup> we examine the narrowest 15 nm wells with the thinnest 10 nm  $\text{Al}_{0.9}\text{Ga}_{0.1}\text{As}$  barrier (see Fig. 1). References 32,33 observed a jump in the drag transresistivity around temperatures  $T \sim 0.2 - 1 \text{ K}$ . A sudden jump can be a signature of a superfluid transition,<sup>34</sup> but the observed deviations were not monotonic, sometimes even changing sign, so any signature of condensation was ambiguous.

We start with the Hamiltonian,

$$\mathcal{H} = \sum_{\mathbf{k}} \xi_{\mathbf{k}}^{\ell} c_{\mathbf{k}}^{\ell\dagger} c_{\mathbf{k}}^{\ell} + \frac{1}{2} \sum_{\substack{\ell \neq \ell', \\ \mathbf{q}, \mathbf{k}, \mathbf{k}'}} V_{\mathbf{k}-\mathbf{k}'}^{\ell\ell'} c_{\mathbf{k}+\frac{\mathbf{q}}{2}}^{\ell\dagger} c_{-\mathbf{k}+\frac{\mathbf{q}}{2}}^{\ell'} c_{-\mathbf{k}'+\frac{\mathbf{q}}{2}}^{\ell} c_{\mathbf{k}'+\frac{\mathbf{q}}{2}}^{\ell'}, \quad (1)$$

where  $c_{\mathbf{k}}^{\ell\dagger}$  and  $c_{\mathbf{k}}^{\ell}$  are creation and destruction operators with label  $\ell = e$  ( $h$ ) for electrons (holes) in their respective quantum wells, and  $\xi_{\mathbf{k}}^{\ell} = k^2/(2m_{\ell}^*) - \mu^{\ell}$  are the single-particle energy band dispersion, with chemical potentials  $\mu^{\ell}$ . While spin-orbit interactions<sup>37</sup> are in general important for the hole bands in GaAs, here they can be neglected because narrow wells suppress Rashba and Dresselhaus interactions due to the large light-hole heavy-hole splitting. Furthermore, the electric fields across the well here are small and the hole densities of interest here are low. The  $V_{\mathbf{k}-\mathbf{k}'}^{\ell\ell'}$  are the bare Coulomb interaction potentials between electrons and holes confined in their finite width wells  $\ell$  and  $\ell'$ . The full expressions for  $V_{\mathbf{k}-\mathbf{k}'}^{\ell\ell'}$  are found in Sec. S1 of the supplementary material.<sup>38</sup>

The mean-field equations at zero temperature for the superfluid gap  $\Delta_{\mathbf{k}}$  and the average chemical potential  $\mu =$

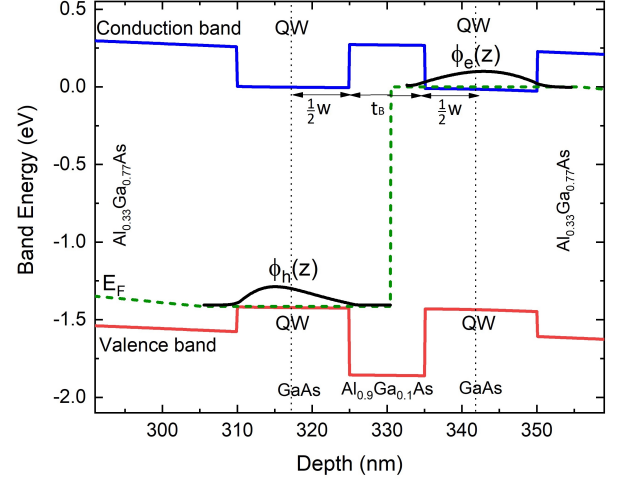


Figure 1. (Color online). Conduction and valence bands for a sample from Ref. 32 in the presence of gate potentials and a bias between the wells,<sup>35</sup> as obtained using a self-consistent Poisson-Schrödinger solver:<sup>36</sup> quantum well widths:  $w = 15 \text{ nm}$  and  $\text{Al}_{0.9}\text{Ga}_{0.1}\text{As}$  barrier thickness:  $t_B = 10 \text{ nm}$ . Dashed green line: Fermi level  $E_F$ . Vertical back dotted lines mark the centers of the wells.  $\phi_e(z)$  and  $\phi_h(z)$  are the resulting electron and hole single-particle wave-functions confined in the wells. Note that the separation of the peaks in the  $\phi_e(z)$  and  $\phi_h(z)$  is larger than the distance between the centers of the two wells.

$(\mu^e + \mu^h)/2$ , for equal electron and hole densities  $n$  are,

$$\Delta_{\mathbf{k}} = -\frac{1}{A} \sum_{\mathbf{k}'} V_{\mathbf{k}-\mathbf{k}'}^{sc} \frac{\Delta_{\mathbf{k}'}}{2E_{\mathbf{k}'}} , \quad (2)$$

$$n = \frac{2}{A} \sum_{\mathbf{k}} (v_{\mathbf{k}})^2 , \quad (3)$$

where  $A$  is the sample surface area,  $E_{\mathbf{k}} = \sqrt{\xi_{\mathbf{k}}^2 + \Delta_{\mathbf{k}}^2}$  with  $\xi_{\mathbf{k}} = \frac{1}{2}(\xi_{\mathbf{k}}^e + \xi_{\mathbf{k}}^h)$ , and the Bogoliubov coherence factors are,

$$u_{\mathbf{k}}^2 = \frac{1}{2} \left( 1 + \frac{\xi_{\mathbf{k}}}{E_{\mathbf{k}}} \right); \quad v_{\mathbf{k}}^2 = \frac{1}{2} \left( 1 - \frac{\xi_{\mathbf{k}}}{E_{\mathbf{k}}} \right). \quad (4)$$

$V_{\mathbf{q}}^{sc}$  is the static screened electron-hole Coulomb interaction in the superfluid state for momentum transfer  $\mathbf{q}$ , evaluated within the Random Phase Approximation (RPA) for electrons and holes of unequal masses. The superfluid energy gap  $\Delta$  near the Fermi surface blocks excitations from the Fermi sea with energies less than  $\Delta$ . This weakens the effect of screening, since low-lying excitations are those needed to screen the long-range Coulomb interactions. The small- $\mathbf{q}$  suppression of screening leads to strong electron-hole pairing peaked at small- $\mathbf{q}$ , and this can lead to large superfluid gaps. The expressions for  $V_{\mathbf{q}}^{sc}$  are given in Sec. S2 of the supplementary material.<sup>38</sup>

A comparison of the good agreement of zero-T superfluid properties for a double layer electron-hole system calculated using the present mean-field RPA approach,<sup>26</sup> with the corresponding results calculated using diffusion quantum Monte

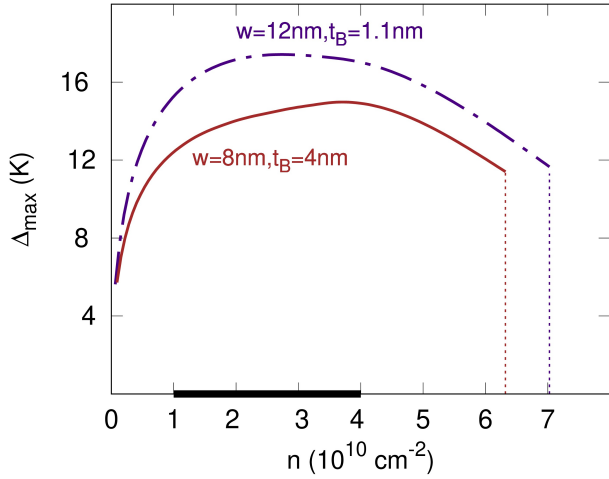


Figure 2. (Color online).  $\Delta_{\max}$  is the maximum value of the zero- $T$  momentum-dependent superfluid gap as a function of  $n$ , the equal electron and hole densities. Solid red line:  $w = 8$  nm and  $t_B = 4$  nm (sample: Refs. 28–30); dash-dot purple line:  $w = 12$  nm and  $t_B = 1.1$  nm (sample: Ref. 31). The horizontal black bar indicates the density range over which anomalous behavior was observed in Refs. 28–30.

Carlo,<sup>27</sup> indicates that the present RPA approach should be a quantitatively good approximation.

For a quasi-two-dimensional system, the superfluid transition is a topological transition associated with the Berezinskii-Kosterlitz-Thouless (BKT) transition temperature<sup>39</sup> which depends only on the superfluid stiffness  $\rho_s(T)$ :<sup>40</sup>  $T^{BKT} = (\pi/2)\rho_s(T^{BKT})$ . Provided  $T^{BKT} \ll \Delta(T=0)$ , which is the case here,  $T^{BKT} \simeq n [\pi\hbar^2/(8(m_e^* + m_h^*))]$ .

Figure 2 shows  $\Delta_{\max}$ , the maximum of the zero- $T$  momentum-dependent gap  $\Delta_{\mathbf{k}}$  determined from Eq. (2), as a function of  $n$ , the equal electron and hole densities for the GaAs heterostructures used for the optical observations<sup>28–31</sup>. Figure 2 illustrates that electron-hole superfluidity is a low-density phenomenon: at higher densities, strong screening greatly weakens the electron-hole coupling, leading to  $\Delta_{\max}$  of, at most, only a few mK<sup>4,41</sup>. In a real system, such small  $\Delta_{\max}$  would be destroyed by disorder. As the density is reduced to  $n_0$ , the onset density,  $\Delta_{\max}$  jumps to energies  $\gtrsim 5$  K. This is a self-consistent effect since large gaps weaken the screening. In Fig. 2, the onset densities are relatively high,  $n_0 \sim 6 - 7 \times 10^{10} \text{ cm}^{-2}$ , thanks to the narrow wells and barriers of the samples in these experiments. For narrower wells and barriers, the average separation between electrons and holes is smaller which strengthens the pairing interactions. The range of densities at which anomalous behavior was observed in Refs. 28–30 is indicated as the green bar on the figure. We note that this lies within the density range for which we predict superfluidity. This adds independent credence that the observed anomalous behavior is indeed associated with superfluidity. We find the maximum Berezinskii-Kosterlitz-Thouless transition temperature is a few Kelvin.

In Sec. S3 of the supplementary material<sup>38</sup> we discuss the

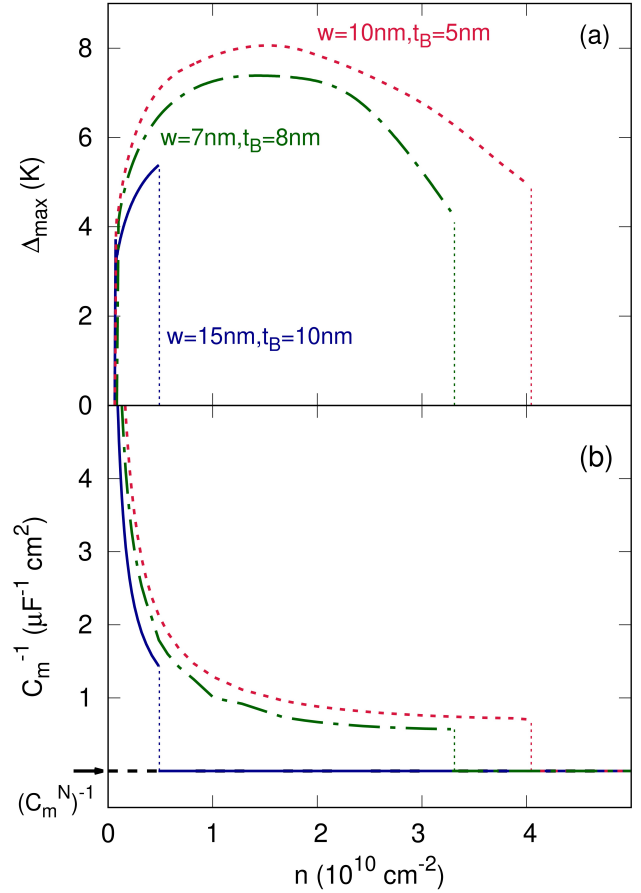


Figure 3. (a)  $\Delta_{\max}$  as a function of  $n$ . Solid blue line:  $w = 15$  nm and  $t_B = 10$  nm (sample: Ref. 32); dash-dot green line:  $w = 7$  nm and  $t_B = 8$  nm; dotted red line:  $w = 10$  nm and  $t_B = 5$  nm. (b) Corresponding inverse of total capacitance  $C_m^{-1}$  as a function of density  $n$ . The inverse of total capacitance in the normal state,  $(C_m^N)^{-1}$ , is indicated.

property that the superfluidity in the GaAs system is nearly always confined within the crossover regime that separates the BCS regime from the BEC regime. This is due to the strong screening that kills superfluidity in the weakly-interacting BCS regime, and to the large electron-hole mass difference in GaAs that impedes the system at low densities from entering the strongly-interacting BEC regime.

As we have discussed, to get high enough mobilities to avoid localization and allow transport studies, the wells and the barriers need to be wider for the transport drag measurements<sup>32,33</sup> compared with the samples for the optical measurements. We see in Fig. 3(a), showing  $\Delta_{\max}$  as a function of  $n$ , that for well widths  $w=15$  nm and barrier thickness  $t_B=10$  nm, the onset density  $n_0 \sim 0.5 \times 10^{10} \text{ cm}^{-2}$ , is an order of magnitude smaller than for the optical measurements. Since the lowest density attained in the drag experiments, was  $n \gtrsim 4 \times 10^{10} \gg n_0$ , we conclude that the anomalous behavior reported in the drag experiments is most probably not an

Table I. A: Double quantum well structure from Ref. 32; B: same structure, calculated without band bending; C: same structure, calculated for the same  $d_c$  but with the width of the quantum wells neglected; D: A different double quantum well structure with the same  $d_c$  as A.

Columns:  $w$  quantum well widths,  $t_B$  barrier thickness,  $d_c$  distance between centers of the two wells,  $d_p$  distance between the peaks of the electron and hole density distributions,  $n_0$  superfluid onset density with  $r_0$  the corresponding average inter-electron spacing,  $\bar{\Delta}$  the maximum value of  $\Delta_{max}$  across all densities, and  $T^{BKT}$  maximum superfluid transition temperature.

	$w$ (nm)	$t_B$ (nm)	$d_c$ (nm)	$d_p$ (nm)	$n_0(10^{10})$ $\text{cm}^{-2}$	$r_0/d_p$	$\bar{\Delta}$ (K)	$T^{BKT}$ (K)
<b>A</b>	15	10	25	27	0.5	3.0	5.2	0.1
<b>B</b>	15	10	25	25	0.8	2.5	6.2	0.3
<b>C</b>	15	10	25	25	1.0	2.3	8.3	0.4
<b>D</b>	10	15	25	29	0.4	3.1	4.0	0.1

indication of a superfluid transition.

Figure 3(a) shows the onset density could be markedly increased to reach the minimum densities attained in Ref. 32, by relatively minor reductions in  $w$  and  $t_B$ . However, interface roughness scattering increases rapidly as the well is made narrower, resulting in samples with very low mobilities. Nevertheless, even if no macroscopically connected superfluid remained, superfluidity may well survive in pockets randomly distributed along the quantum wells. Such pockets of superfluidity could be detected using capacitance spectroscopy.<sup>42</sup>

In capacitance spectroscopy, a low frequency ac voltage is delivered to a top gate with the quantum wells grounded. The total capacitance  $C_m = (C_g^{-1} + C_Q^{-1})^{-1}$  between the gate and quantum wells is measured.  $C_g$  is the classical geometry capacitance per unit area which depends only on the sample structure.  $C_Q = e^2 \partial n / \partial \mu$  is the quantum capacitance and is proportional to the density of states. For a two-dimensional system in the normal state  $C_Q^N = (1/A)[e^2 m^* / (\pi \hbar^2)]$ , inversely proportional to the sample area. For a pocket of superfluidity of area  $A' \leq A$ , the quantum capacitance is,

$$C_Q^S = \frac{1}{A'} \left[ e^2 \sum_{\mathbf{k}} \delta(\mu - \epsilon_F) + 4e^2 \sum_{\mathbf{k}} \frac{u_{\mathbf{k}}^2 v_{\mathbf{k}}^2}{E_{\mathbf{k}}} \right]. \quad (5)$$

$C_Q^S < C_Q^N$ , because of the gap in the low-lying energy spectrum.<sup>42,43</sup>

Figure 3(b) shows the inverse of the total capacitance  $C_m^{-1}$  as a function of density for homogeneous systems. From Fig. 3(a), the onset density for superfluidity for well widths  $w = 10$  nm and barrier thickness  $t_B = 5$  nm, is  $n_0 \sim 4 \times 10^{10} \text{ cm}^{-2}$ .  $C_m^N$  is the corresponding total capacitance in the normal state. The onset of superfluidity is characterised by a jump in  $C_m^{-1}$  at  $n_0$ , and  $C_m^{-1}$  monotonically increases as the density is further decreased. For the inhomogeneous system with pockets of superfluid of total area  $A'$ , the behavior would be similar, but the jump in  $C_m^{-1}$  at  $n_0$  would be reduced by an amount proportional to  $(A'/A)$ .

Table I shows the effects on the superfluid properties of band bending and the finite width of the quantum wells for

samples from Ref. 32. We saw in Fig. 1 that band bending pushes the peaks of the electron and hole density distributions ( $d_p$ ) further apart than the distance between the centers of the wells ( $d_c$ ). The effect of this in weakening the superfluidity can be seen by comparing rows A and B. In row B, band bending has been neglected. The finite thickness of the wells also weakens the superfluidity. This can be seen by comparing row A with row C, calculated for the same  $d_c$  but neglecting the well widths. For a fixed distance between the centers of the wells  $d_c$ , narrower wells with a thicker barrier also weaken the superfluidity, a combined effect of banding bending and the gate potentials.<sup>35</sup> This is seen by comparing rows A and D. The ratio  $r_0/d_p$ , where  $r_0$  is the average spacing of the electrons at the superfluid onset density  $n_0$ , is a useful indicator of the effect of the heterostructure parameters on  $n_0$ . The table shows that  $n_0$  occurs for a value of the ratio  $r_0/d_p \sim 2.5 - 3$ . For smaller  $r_0$ , the screening is too strong and the superfluidity cannot overcome the screening.

The unusually large effective mass difference between electrons and holes in GaAs makes experimental realization of superfluidity in GaAs double quantum wells a particularly worthwhile goal, likely to reveal intriguing new physics. While in principle this physics can also be investigated with ultracold atoms of different masses, the exotic superfluid phases are predicted for the ultracold atom system only below nanoKelvin temperatures, whereas for GaAs the transition temperatures are a few Kelvin. The primary reason it has proved so difficult to observe superfluidity in GaAs is that the phenomenon only occurs at low densities, due to strong screening at higher densities of the long-range Coulomb pairing interactions. Screening kills superfluidity above an onset density. To generate superfluidity in GaAs at accessible experimental densities requires narrow quantum wells and thin barriers that have been impractical for transport experiments because of the very low mobility of the samples. However, we show that inhomogeneous pockets of superfluidity could be detected in samples of low mobility using standard capacitance measurement techniques. Finally, our calculations confirm that superfluid condensation of optically generated electron-hole pairs is indeed feasible with existing experimental samples.

**Acknowledgments.** We thank Kanti Das Gupta, François Dubin, Ugo Siciliani de Cumis, Michele Pini, and Joanna Waldie for illuminating discussions. This work was partially supported by the Flemish Science Foundation (FWO-VI), and the Australian Government through the Australian Research Council Centre of Excellence in Future Low-Energy Electronics (Project No. CE170100039).

# I. SUPPLEMENTARY MATERIAL

## EXPERIMENTAL CONDITIONS FOR OBSERVATION OF ELECTRON-HOLE SUPERFLUIDITY IN GAAS HETEROSTRUCTURES

### S1. BARE COULOMB INTERACTIONS

The  $V_{\mathbf{k}-\mathbf{k}'}^{\ell\ell'}$  are the bare Coulomb interaction potentials between electrons and holes confined in their wells  $\ell$  and  $\ell'$ ,

$$\begin{aligned} V_{\mathbf{k}-\mathbf{k}'}^{\ell\ell} &= \frac{2\pi e^2}{\epsilon} \frac{1}{|\mathbf{k}-\mathbf{k}'|} F_{\mathbf{k}-\mathbf{k}'}^{\ell\ell}; \\ V_{\mathbf{k}-\mathbf{k}'}^{\ell\neq\ell'} &= -\frac{2\pi e^2}{\epsilon} \frac{e^{-d|\mathbf{k}-\mathbf{k}'|}}{|\mathbf{k}-\mathbf{k}'|} F_{\mathbf{k}-\mathbf{k}'}^{\ell\ell'}. \end{aligned} \quad (\text{S1})$$

$V_{\mathbf{k}-\mathbf{k}'}^{\ell\ell}$  is the bare intralayer interaction and  $V_{\mathbf{k}-\mathbf{k}'}^{\ell\neq\ell'}$  the bare interlayer interaction. We take the dielectric constant for GaAs and  $\text{Al}_{0.9}\text{Ga}_{0.1}\text{As}$  as  $\epsilon = 12.9$ . We consider only wells of equal width  $w$ , separated by a  $\text{Al}_{0.9}\text{Ga}_{0.1}\text{As}$  insulating barrier of thickness  $t_B$ . We express lengths in units of the effective Bohr radius,  $a_B^* = \hbar^2 4\pi\epsilon_0\epsilon / (m^* e^2) = 12.5$  nm for GaAs, and energies in effective Rydbergs,  $\text{Ry}^* = e^2 / (2a_B^*) = 4.5$  meV = 52 K for GaAs.  $m^*$  is the reduced effective mass.

The form-factors in Eq. (S1),

$$F_{\mathbf{q}}^{\ell\ell'} = \int_{-\infty}^{\infty} dz \int_{-\infty}^{\infty} dz' |\phi_{\ell}(z)|^2 |\phi_{\ell'}(z')|^2 \exp(-q|z-z'|), \quad (\text{S2})$$

account for the confinement of the electrons and holes in their finite-width quantum wells.  $\phi_{\ell}(z)$  is the wave-function of the

electron or hole (see Fig. 1 of main manuscript). The  $\phi_{\ell}(z)$  are evaluated numerically using a self-consistent Poisson-Schrödinger solver.<sup>36</sup> They are sensitive to the voltages on the front and back gates that are used to independently tune the populations in the well. The  $\phi_{\ell}(z)$  are also sensitive to any external interlayer bias. In the optical measurements, an electric field across the barrier spatially separates the optically generated electrons and holes into opposite wells, while in the transport drag measurements a bias is used to offset the different electrochemical potentials of the holes and electrons.<sup>32,33,44</sup>

### S2. SCREENED COULOMB INTERACTION IN SUPERFLUID STATE

In the normal state, the static screened electron-hole Coulomb interaction evaluated within the Random Phase Approximation (RPA) for electrons and holes of unequal masses is,<sup>45</sup>

$$V_{\mathbf{q}}^{sc} = \frac{V_{\mathbf{q}}^{eh}}{[1 - V_{\mathbf{q}}^{ee}\Pi_0^e(\mathbf{q})][1 - V_{\mathbf{q}}^{hh}\Pi_0^h(\mathbf{q})] - [V_{\mathbf{q}}^{eh}]^2\Pi_0^e(\mathbf{q})\Pi_0^h(\mathbf{q})}} \quad (\text{S3})$$

where

$$\Pi_0^{\ell}(\mathbf{q}) = 2 \sum_{\mathbf{k}} \frac{f_{FD}(\xi_{\mathbf{k}-\mathbf{q}}^{\ell}) - f_{FD}(\xi_{\mathbf{k}}^{\ell})}{\xi_{\mathbf{k}-\mathbf{q}}^{\ell} - \xi_{\mathbf{k}}^{\ell}} \quad (\text{S4})$$

is the Lindhard particle-hole polarization in well  $\ell$ .  $f_{FD}(x)$  is the zero- $T$  Fermi-Dirac distribution function.

In the superfluid state, the expression for the static RPA electron-hole Coulomb interaction  $V_{\mathbf{q}}^{sc}$  is different,<sup>41,46,47</sup>

$$V_{\mathbf{q}}^{sc} = \frac{V_{\mathbf{q}}^{eh} + \Pi_a(\mathbf{q})[V_{\mathbf{q}}^{ee}V_{\mathbf{q}}^{hh} - (V_{\mathbf{q}}^{eh})^2]}{1 - \Pi_n(\mathbf{q})[V_{\mathbf{q}}^{ee} + V_{\mathbf{q}}^{hh}] + 2V_{\mathbf{q}}^{eh}\Pi_a(\mathbf{q}) + [V_{\mathbf{q}}^{ee}V_{\mathbf{q}}^{hh} - (V_{\mathbf{q}}^{eh})^2][\Pi_n^2(\mathbf{q}) - \Pi_a^2(\mathbf{q})]}, \quad (\text{S5})$$

where  $\Pi_n(\mathbf{q})$  is the normal polarizability, modified from the polarizabilities in Eq. (S4) for the normal state by the presence of the superfluid gap in the energy spectrum,

$$\begin{aligned} \Pi_n(\mathbf{q}) &= 2 \sum_{\mathbf{k}} \left[ u_{\mathbf{k}}^2 u_{\mathbf{k}-\mathbf{q}}^2 \frac{f_{FD}(E_{\mathbf{k}-\mathbf{q}}^+) - f_{FD}(E_{\mathbf{k}}^+)}{E_{\mathbf{k}-\mathbf{q}}^+ - E_{\mathbf{k}}^+} + v_{\mathbf{k}}^2 v_{\mathbf{k}-\mathbf{q}}^2 \frac{f_{FD}(E_{\mathbf{k}-\mathbf{q}}^-) - f_{FD}(E_{\mathbf{k}}^-)}{E_{\mathbf{k}-\mathbf{q}}^- - E_{\mathbf{k}}^-} \right. \\ &\quad \left. - u_{\mathbf{k}}^2 v_{\mathbf{k}-\mathbf{q}}^2 \frac{1 - f_{FD}(E_{\mathbf{k}-\mathbf{q}}^-) - f_{FD}(E_{\mathbf{k}}^+)}{E_{\mathbf{k}-\mathbf{q}}^- + E_{\mathbf{k}}^+} - v_{\mathbf{k}}^2 u_{\mathbf{k}-\mathbf{q}}^2 \frac{1 - f_{FD}(E_{\mathbf{k}-\mathbf{q}}^+) - f_{FD}(E_{\mathbf{k}}^-)}{E_{\mathbf{k}-\mathbf{q}}^+ + E_{\mathbf{k}}^-} \right], \end{aligned} \quad (\text{S6})$$

with  $E_{\mathbf{k}}^{\pm} = E_{\mathbf{k}} \pm \delta\xi_{\mathbf{k}}$  and  $\delta\xi_{\mathbf{k}} = \frac{1}{2}(\xi_{\mathbf{k}}^e - \xi_{\mathbf{k}}^h)$ , and  $\Pi_a(\mathbf{q})$  is the anomalous polarizability,<sup>4,41</sup>

$$\begin{aligned} \Pi_a(\mathbf{q}) &= 2 \sum_{\mathbf{k}} u_{\mathbf{k}} v_{\mathbf{k}-\mathbf{q}} v_{\mathbf{k}} u_{\mathbf{k}-\mathbf{q}} \left[ \frac{f_{FD}(E_{\mathbf{k}-\mathbf{q}}^+) - f_{FD}(E_{\mathbf{k}}^+)}{E_{\mathbf{k}-\mathbf{q}}^+ - E_{\mathbf{k}}^+} - \frac{f_{FD}(E_{\mathbf{k}-\mathbf{q}}^-) - f_{FD}(E_{\mathbf{k}}^-)}{-E_{\mathbf{k}-\mathbf{q}}^- + E_{\mathbf{k}}^-} \right. \\ &\quad \left. + \frac{1 - f_{FD}(E_{\mathbf{k}-\mathbf{q}}^-) - f_{FD}(E_{\mathbf{k}}^+)}{E_{\mathbf{k}-\mathbf{q}}^- + E_{\mathbf{k}}^+} + \frac{1 - f_{FD}(E_{\mathbf{k}-\mathbf{q}}^+) - f_{FD}(E_{\mathbf{k}}^-)}{E_{\mathbf{k}-\mathbf{q}}^+ + E_{\mathbf{k}}^-} \right]. \end{aligned} \quad (\text{S7})$$

Equations S5-S7 include the effect of the unequal masses.

The full polarization is  $\Pi_0(\mathbf{q}) = \Pi_n(\mathbf{q}) + \Pi_a(\mathbf{q})$ . In the

normal state  $\Pi_a(\mathbf{q}) = 0$ . In the superfluid state  $\Pi_a(0) = -\Pi_n(0)$  so  $\Pi_0(0) = 0$ , and  $\Pi_0(\mathbf{q})$  is suppressed for small  $\mathbf{q}$  by the presence of the gap in the energy spectrum.<sup>48,49</sup>

### S3. CONDENSATE FRACTION, CHEMICAL POTENTIAL AND INTRAPAIR CORRELATION LENGTH

The superfluid BCS, BCS-BEC crossover and BEC regimes can be characterized by the condensate fraction  $c$ , the fraction of carriers bound in pairs.<sup>50,51</sup> For  $c \leq 0.2$  the superfluid condensate is in the BCS regime, for  $0.2 < c < 0.8$  in the crossover regime, and for  $c \geq 0.8$  in the BEC regime. In Fig. S1(a) we see the condensate fraction  $c$  as a function of density, for a sample with well widths  $w = 8$  nm and barrier thickness  $t_B = 4$  nm. The figure shows that the superfluidity is essentially always confined to the crossover regime. At the superfluid onset density  $n_0 \sim 6.3 \times 10^{10} \text{ cm}^{-2}$ ,  $c$  drops sharply from  $c = 0.36$  to exponentially small values (see Ref. 26 and the discussion of the behavior of  $\Delta_{max}$  near  $n_0$  in the main manuscript). A value of 0.36 implies that when the superfluidity starts it is in the crossover region. Strong screening kills superfluidity in the BCS regime.

It is also difficult for the system to enter the BEC regime at low densities, a consequence of the large mass difference: even for pairs compact on the scale of the interparticle spacing, the electrons and holes in the pairs can still respond and screen an electric field.

Fig. S1(b) and (c) show as a function of density, the chemical potential  $\mu$  and the intra pair correlation length  $\xi$ , defined as the radius of an isolated electron-hole bound pair.<sup>52</sup> Above the onset density, the system is in the normal state and  $\mu$  is equal to the Fermi energy.  $\mu$  drops at the onset density, but it only reaches negative values, corresponding to the deep BEC

regime, at extremely low density. Similarly,  $\xi$  only drops to the effective Bohr radius  $a_B^*$  at low density.

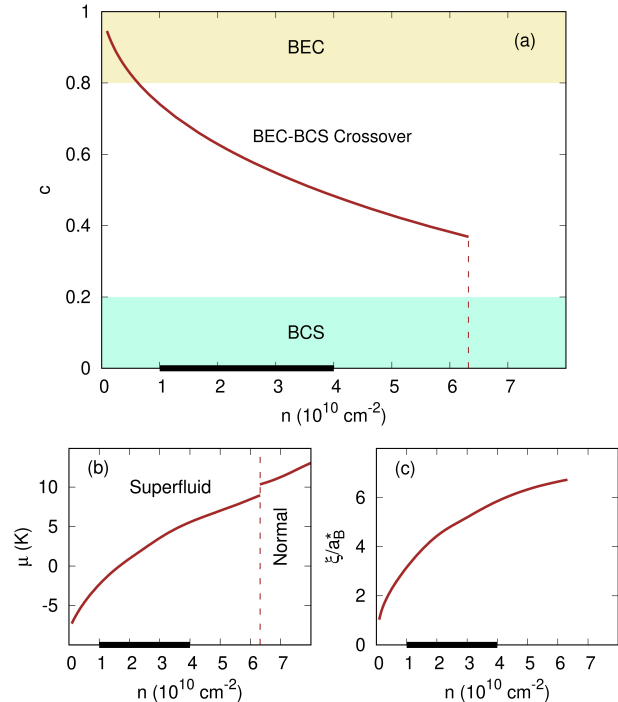


Figure S1. (a) Condensate fraction  $c$  as a function of equal electron and hole densities  $n$ , for a double quantum well in GaAs with well widths  $w = 8$  nm and barrier thickness  $t_B = 4$  nm (sample: Refs. 28–30). The superfluid onset density is  $n_0 = 6.3 \times 10^{10} \text{ cm}^{-2}$ , indicated by vertical dashed line. (b) Corresponding chemical potential  $\mu$ . (c) Corresponding intra pair correlation length  $\xi$ .  $a_B^*$  is the effective Bohr radius. The horizontal black bar indicates the density range over which anomalous behavior was observed in Refs. 28–30.

- <sup>1</sup> M. Bartenstein, A. Altmeyer, S. Riedl, S. Jochim, C. Chin, J. Hecker Denschlag, and R. Grimm, “Crossover from a molecular Bose-Einstein Condensate to a degenerate Fermi gas,” *Phys. Rev. Lett.* **92**, 120401 (2004).
- <sup>2</sup> C. A. Regal, M. Greiner, and D. S. Jin, “Observation of resonance condensation of fermionic atom pairs,” *Phys. Rev. Lett.* **92**, 040403 (2004).
- <sup>3</sup> M. W. Zwierlein, C. A. Stan, C. H. Schunck, S. M. F. Raupach, A. J. Kerman, and W. Ketterle, “Condensation of pairs of fermionic atoms near a Feshbach resonance,” *Phys. Rev. Lett.* **92**, 120403 (2004).
- <sup>4</sup> A. Perali, D. Neilson, and A. R. Hamilton, “High-temperature superfluidity in double-bilayer graphene,” *Phys. Rev. Lett.* **110**, 146803 (2013).
- <sup>5</sup> S. Conti, M. Van der Donck, A. Perali, F. M. Peeters, and D. Neilson, “A doping-dependent switch from one- to two-component superfluidity at temperature above 100K in coupled electron-hole Van der Waals heterostructures,” (2019), [arXiv:1909.03411 \[cond-mat.supr-con\]](https://arxiv.org/abs/1909.03411).
- <sup>6</sup> G. W. Burg, N. Prasad, K. Kim, T. Taniguchi, K. Watanabe, A. H. MacDonald, L. F. Register, and E. Tutuc, “Strongly enhanced

- tunneling at total charge neutrality in double-bilayer graphene-WSe<sub>2</sub> heterostructures,” *Phys. Rev. Lett.* **120**, 177702 (2018).
- <sup>7</sup> D. K. Efimkin, G. W. Burg, E. Tutuc, and A. H. MacDonald, “Tunneling and fluctuating electron-hole Cooper pairs in double bilayer graphene,” [arXiv:1903.07739v1 \[cond-mat.mes-hall\]](https://arxiv.org/abs/1903.07739v1) (2019).
- <sup>8</sup> Z. Wang, D. A. Rhodes, K. Watanabe, T. Taniguchi, J. C. Hone, J. Shan, and K. F. Mak, “Evidence of high-temperature exciton condensation in two-dimensional atomic double layers,” *Nature* **574**, 76 (2019).
- <sup>9</sup> A. Chaves and D. Neilson, “Two-dimensional semiconductors host high-temperature exotic state,” *Nature* **574**, 39 (2019).
- <sup>10</sup> I. B. Spielman, J. P. Eisenstein, L. N. Pfeiffer, and K. W. West, “Resonantly enhanced tunneling in a double layer quantum Hall ferromagnet,” *Phys. Rev. Lett.* **84**, 5808 (2000).
- <sup>11</sup> C. Comte and P. Nozières, “Exciton Bose condensation : The ground state of an electron-hole gas - I. Mean field description of a simplified model,” *J. Phys. France* **43**, 1069 (1982).
- <sup>12</sup> L. V. Keldysh and Y. V. Kopayev, “Possible instability of semimetallic state toward Coulomb interaction,” *Sov. Phys. Solid State* **6**, 2219 (1965).

- <sup>13</sup> L. V. Keldysh and Y. V. Kopaev, "Collective properties of excitons in semiconductors," *Sov. Phys. JETP* **27**, 521 (1968).
- <sup>14</sup> Y. E. Lozovik and V. I. Yudson, "Feasibility of superfluidity of paired spatially separated electrons and holes," *JETP Lett* **22**, 274 (1975), (*Pisma Zh. Eksp. Teor. Fiz.* **22**, 556 (1975)).
- <sup>15</sup> Y. E. Lozovik and V. I. Yudson, "A new mechanism for superconductivity: pairing between spatially separated electrons and holes," *Zh. Eksp. Teor. Fiz* **71**, 738 (1976), (*Sov. Phys. JETP* **44**, 389 (1976)).
- <sup>16</sup> S. Conti, A. Perali, F. M. Peeters, and D. Neilson, "Multicomponent screening and superfluidity in gapped electron-hole double bilayer graphene with realistic bands," *Phys. Rev. B* **99**, 144517 (2019).
- <sup>17</sup> S. Saberi-Pouya, M. Zarenia, A. Perali, T. Vazifehshenas, and F. M. Peeters, "High-temperature electron-hole superfluidity with strong anisotropic gaps in double phosphorene monolayers," *Phys. Rev. B* **97**, 174503 (2018).
- <sup>18</sup> C. Ravensbergen, V. Corre, E. Soave, M. Kreyer, E. Kirilov, and R. Grimm, "Production of a degenerate Fermi-Fermi mixture of dysprosium and potassium atoms," *Phys. Rev. A* **98**, 063624 (2018).
- <sup>19</sup> P. Pieri, D. Neilson, and G. C. Strinati, "Effects of density imbalance on the BCS-BEC crossover in semiconductor electron-hole bilayers," *Phys. Rev. B* **75**, 113301 (2007).
- <sup>20</sup> J. J. Kinnunen, J. E. Baarsma, J.-P. Martikainen, and P. Trm, "The Fulde-Ferrell-Larkin-Ovchinnikov state for ultracold fermions in lattice and harmonic potentials: a review," *Rep. Prog. Phys.* **81**, 046401 (2018).
- <sup>21</sup> B. Frank, J. Lang, and W. Zwerger, "Universal phase diagram and scaling functions of imbalanced Fermi gases," *J. Exp. Theor. Phys.* **127**, 812 (2018).
- <sup>22</sup> J. Wang, Y. Che, L. Zhang, and Q. Chen, "Enhancement effect of mass imbalance on Fulde-Ferrell-Larkin-Ovchinnikov type of pairing in Fermi-Fermi mixtures of ultracold quantum gases," *Sci. Rep.* **7**, 39783 (2017).
- <sup>23</sup> M. M. Forbes, E. Gubankova, W. V. Liu, and F. Wilczek, "Stability criteria for breached-pair superfluidity," *Phys. Rev. Lett.* **94**, 017001 (2005).
- <sup>24</sup> J. E. Baarsma and H. T. C. Stoof, "Inhomogeneous superfluid phases in  ${}^6\text{Li}$ - ${}^{40}\text{K}$  mixtures at unitarity," *Phys. Rev. A* **87**, 063612 (2013).
- <sup>25</sup> Y.-C. Zhang, F. Maucher, and T. Pohl, "Supersolidity around a critical point in dipolar Bose-Einstein condensates," *Phys. Rev. Lett.* **123**, 015301 (2019).
- <sup>26</sup> D. Neilson, A. Perali, and A. R. Hamilton, "Excitonic superfluidity and screening in electron-hole bilayer systems," *Phys. Rev. B* **89**, 060502 (2014).
- <sup>27</sup> P. López Ríos, A. Perali, R. J. Needs, and D. Neilson, "Evidence from quantum Monte Carlo simulations of large-gap superfluidity and BCS-BEC crossover in double electron-hole layers," *Phys. Rev. Lett.* **120**, 177701 (2018).
- <sup>28</sup> L. V. Butov, A. C. Gossard, and D. S. Chemla, "Macroscopically ordered state in an exciton system," *Nature* **418**, 751 (2002).
- <sup>29</sup> A. A. High, J. R. Leonard, M. Remeika, L. V. Butov, M. Hanson, and A. C. Gossard, "Condensation of excitons in a trap," *Nano Lett.* **12**, 2605 (2012).
- <sup>30</sup> R. Anankine, M. Beian, S. Dang, M. Alloing, E. Cambril, K. Merghem, C. G. Carbonell, A. Lemaître, and F. Dubin, "Quantized vortices and four-component superfluidity of semiconductor excitons," *Phys. Rev. Lett.* **118**, 127402 (2017).
- <sup>31</sup> V. B. Timofeev and A. V. Gorbunov, "Collective state of the Bose gas of interacting dipolar excitons," *J. Appl. Phys.* **101**, 081708 (2007).
- <sup>32</sup> A. F. Croxall, K. Das Gupta, C. A. Nicoll, M. Thangaraj, H. E. Beere, I. Farrer, D. A. Ritchie, and M. Pepper, "Anomalous Coulomb drag in electron-hole bilayers," *Phys. Rev. Lett.* **101**, 246801 (2008).
- <sup>33</sup> J. A. Seamons, C. P. Morath, J. L. Reno, and M. P. Lilly, "Coulomb drag in the exciton regime in electron-hole bilayers," *Phys. Rev. Lett.* **102**, 026804 (2009).
- <sup>34</sup> G. Vignale and A. H. MacDonald, "Drag in paired electron-hole layers," *Phys. Rev. Lett.* **76**, 2786 (1996).
- <sup>35</sup> B. Zheng, A. F. Croxall, J. Waldie, K. Das Gupta, F. Sfigakis, I. Farrer, H. E. Beere, and D. A. Ritchie, "Switching between attractive and repulsive Coulomb-interaction-mediated drag in an ambipolar GaAs/AlGaAs bilayer device," *Appl. Phys. Lett.* **108**, 062102 (2016).
- <sup>36</sup> I. H. Tan, G. L. Snider, L. D. Chang, and E. L. Hu, "A self-consistent solution of Schrödinger-Poisson equations using a nonuniform mesh," *J. Appl. Phys.* **68**, 4071 (1990).
- <sup>37</sup> E. I. Rashba, "Properties of semiconductors with an extremum loop. I. Cyclotron and combinational resonance in a magnetic field perpendicular to the plane of the loop," *Sov. Phys., Solid State* **2**, 1109 (1960).
- <sup>38</sup> See Supplementary Material.
- <sup>39</sup> J. M. Kosterlitz and D. J. Thouless, "Ordering, metastability and phase transitions in two-dimensional systems," *J. Phys. C: Solid State* **6**, 1181 (1973).
- <sup>40</sup> S. S. Botelho and C. A. R. Sá de Melo, "Vortex-antivortex lattice in ultracold fermionic gases," *Phys. Rev. Lett.* **96**, 040404 (2006).
- <sup>41</sup> Y. E. Lozovik, S. L. Ogarkov, and A. A. Sokolik, "Condensation of electron-hole pairs in a two-layer graphene system: Correlation effects," *Phys. Rev. B* **86**, 045429 (2012).
- <sup>42</sup> L. Du, X. Li, W. Lou, G. Sullivan, K. Chang, J. Kono, and R.-R. Du, "Evidence for a topological excitonic insulator in InAs/GaSb bilayers," *Nat. Commun.* **8**, 1971 (2017).
- <sup>43</sup> M. J. Yang, C. H. Yang, B. R. Bennett, and B. V. Shanabrook, "Evidence of a hybridization gap in "semimetallic" InAs/GaSb systems," *Phys. Rev. Lett.* **78**, 4613 (1997).
- <sup>44</sup> U. Sivan, P. M. Solomon, and H. Shtrikman, "Coupled electron-hole transport," *Phys. Rev. Lett.* **68**, 1196 (1992).
- <sup>45</sup> K. Flensberg and Ben Y.-K. Hu, "Plasmon enhancement of Coulomb drag in double-quantum-well systems," *Phys. Rev. B* **52**, 14796 (1995).
- <sup>46</sup> M. Iskin and C. A. R. Sá de Melo, "Mixtures of ultracold fermions with unequal masses," *Phys. Rev. A* **76**, 013601 (2007).
- <sup>47</sup> I. Sodemann, D. A. Pesin, and A. H. MacDonald, "Interaction-enhanced coherence between two-dimensional Dirac layers," *Phys. Rev. B* **85**, 195136 (2012).
- <sup>48</sup> Z. W. Gortel and L. Świerkowski, "Superfluid ground state in electron-hole double layer systems," *Surf. Sci.* **361**, 146 (1996).
- <sup>49</sup> R. Bistritzer, H. Min, J.-J. Su, and A. H. MacDonald, "Comment on "Electron screening and excitonic condensation in double-layer graphene systems," *ArXiv:cond-mat/0810.0331v1 [cond-mat.mes-hall]* (2008).
- <sup>50</sup> L. Salasnich, N. Manini, and A. Parola, "Condensate fraction of a Fermi gas in the BCS-BEC crossover," *Phys. Rev. A* **72**, 023621 (2005).
- <sup>51</sup> A. Guidini and A. Perali, "Band-edge BCS-BEC crossover in a two-band superconductor: physical properties and detection parameters," *Supercond. Sci. Tech.* **27**, 124002 (2014).
- <sup>52</sup> F. Pistolesi and G. C. Strinati, "Evolution from BCS superconductivity to Bose condensation: Calculation of the zero-temperature phase coherence length," *Phys. Rev. B* **53**, 15168 (1996).